Journal of Engineering Mathematics **31:** 269–284, 1997.

Edge-flames

J. BUCKMASTER
University of Illinois Urbana, IL 61801, U.S.A.

Received 1 April 1996; accepted in revised form 21 October 1996

Abstract. Edge-flames arise in non-premixed combustion, and include the familiar triple, or tribrachial flames. They can exist for all Damköhler numbers for which the upper and lower branches of the S-shaped response of the underlying diffusion flame simultaneously exist, and have negative propagation speeds (corresponding to failure waves) when the Damköhler number is close to the quenching value, positive speeds (corresponding to ignition waves) when the Damköhler number is close to the ignition value. A previously described one-dimensional model of edge-flames is here applied to a number of new situations. These include: a description of unbounded edge-flames, for unit Lewis numbers, over the entire range of Damköhler numbers; a description of unbounded edge-flames when one of the Lewis numbers differs from unity, for which it is shown that propagating edge-flames of stationary structure may not exist; and an analysis of an edge-flame near a wall, without flow between the wall and the flame. In the case of unbounded edge-flames, a simple formula for the edge speed is derived that may be of value in the computation of turbulent combustion fields in the laminar flamelet regime.

Key words: non-premixed combustion, propagation speeds, laminar flamelets

1. Introduction

The essential characteristic of a diffusion flame is that the fuel and oxygen are separated by a reaction zone or flame sheet. In many examples of non-premixed combustion, however, there are regions where the sheet is missing, and mixing will occur there with little or no reaction. The boundaries between regions with sheets and regions without sheets define what we shall call edge-flames.

A simple example of an edge-flame arises when a premixed flame propagates through a mixture weakly stratified in the direction perpendicular to the direction of propagation, and in which there is a level surface of stoichiometry. Excess fuel on the rich side of the surface remains unburnt on passage through the flame, as does excess oxygen on the lean side. These hot reactants then diffuse towards each other and support a diffusion flame that trails behind the premixed flame, [1]. The resulting structure is called a triple flame or a tribrachial flame, the latter emphasizing the 3-armed nature of the configuration – a fuel-rich premixed arm, a fuel-lean premixed arm, and a diffusion arm.

Edge-flames will not always be characterized by a branched structure, although premixing at the edge will often be an important characteristic. Tube-burner flames are edge-flames, since there is a gap between the burner rim and the base of the flame; a flame spreading over a fuel bed, solid or liquid, will have an edge; and candle flames burning at small Grashof number have a well-defined circular edge, [2].

Edge-flames are an important characteristic of turbulent combustion in the flamelet regime. When the Lewis numbers of both fuel and oxygen equal 1, the mixture fraction Z is a conserved scalar. A diffusion flame sheet, if it exists, will be located at the stoichiometric level surface of Z, $Z = Z_{\text{stoich}}$. Since the sheet is thin, its structure is controlled by balances between diffusion and reaction, and when we express these balances using Z as the independent variable, rather

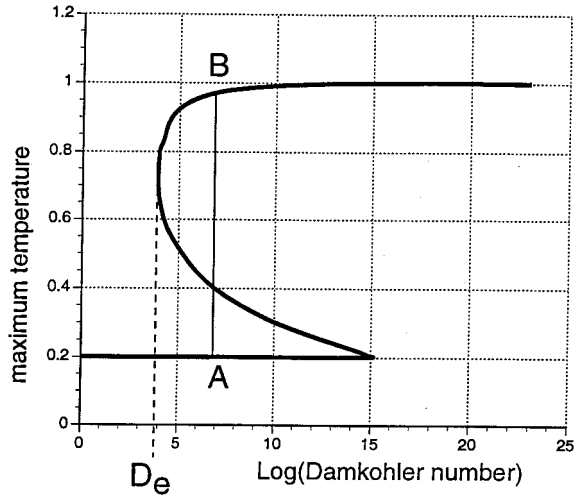

Figure 1. Response of a one-dimensional diffusion flame.

than physical distance, a local Damköhler number is defined that is inversely proportional to χ_{stoich}, the scalar dissipation rate χ evaluated at stoichometry, where

$$\chi = 2D|\nabla Z|^2. \tag{1}$$

If χ_{stoich} is large enough, the Damköhler number can lie below the quenching value, and the sheet is destroyed. Since χ varies both in the mean and stochastically, there will be regions where the sheet can exist, and regions where it cannot, separated by edges. Of course, edge-flames will also arise in turbulent combustion when the Lewis numbers are not equal to 1, but we lack a simple description of the flamelets in that case.

A mathematical framework for edge-flames starts with the familiar S-shaped response of one-dimensional diffusion flames (Figure 1). The upper branch of this response corresponds to vigorous burning with a maximum temperature close to the Burke-Schumann flame temperature. This vigorous burning is characterized by a flame sheet whose role in the overall combustion field is barely distinguishable from that of a Burke-Schumann flame sheet. Specifically, reactant leakage through the sheet is small, varying from zero in the limit of infinite Damköhler number, to $O(\varepsilon)$ at the quenching value D_e, where ε is a characteristic non-dimensional inverse activation energy. The solutions on this branch are characteristic of the post-edge state of an edge-flame.

The lower branch of the response corresponds to stable weak burning. The maximum temperature on this branch is close to the supply or background temperature, and in many practical situations this is so small that the reaction is completely quenched, and only mixing occurs. The solutions on this branch are characteristic of the ante-edge state of an edge-flame.

With these remarks in mind, we can think of a stationary edge-flame as an evolution in space from a solution corresponding to the point A (Figure 1) to a solution corresponding to the point B. This evolution will occur over the entire line ($-\infty$ to $+\infty$) in the case of an unbounded edge-flame, and over the half-line $(0$ to $\infty)$ for a laminar flame on a burner or a flame sitting over a fuel bed. For a burner flame the edge speed is positive relative to the flow of unburnt gas. For the steady small-Grashof-number candle flame the edge speed is zero, but oscillations are observed near extinction corresponding to both positive and negative edge

speeds, [2]. Edge-flames can have negative flame speeds if the Damköhler number is small enough, but edge-flames will not exist if $D < D_e$.

2. A one-dimensional model of edge-flames

Recently, Buckmaster [3] proposed a one-dimensional model of edge flames. This has been used to study unbounded edge-flames and their stability when the Lewis number of one of the reactants is 1, and that of the other differs from 1 by only $O(\varepsilon)$ amounts. It has also been used to examine edge-flame-holding [4] and blow-off. Here we shall re-examine the unbounded problem with both Lewis numbers equal to 1, and show that the formula for the edge-speed is precisely the formula adopted (on physical grounds only) in [5] in a study of lifted turbulent flames; and we shall extend the discussion to a wider range of Damköhler numbers, specifically to values near the quenching value D_e, where edge speeds are large and negative. Also, we shall examine unbounded flames with one Lewis number that is sigificantly different from 1, a non-trivial extension of the earlier work, one which requires modification of the earlier model. Solutions in this case reveal the possibility that, should the Lewis number be greater than 1, there is a range of Damköhler numbers (greater than the quenching value) for which a propagating edge with stationary structure cannot exist. And we shall examine stationary edge-flames near walls, in which there is no gas flow over the edge.

We start with the two-dimensional equations

$$\begin{aligned} &\rho C_p \frac{\partial T}{\partial t} - \lambda \frac{\partial^2 T}{\partial x^2} = S_T + Q\Omega_T, \qquad \rho \frac{\partial X}{\partial t} - \rho D_X \frac{\partial^2 X}{\partial x^2} = S_X - \Omega_X, \\ &\rho \frac{\partial Y}{\partial t} - \rho D_Y \frac{\partial^2 Y}{\partial x^2} = S_Y - \Omega_Y, \end{aligned} \tag{2}$$

where x is the distance measured along the direction in which the A-B evolution of Figure 1 proceeds. The terms S_T, S_X and S_Y are 'side' terms. These terms arise from gradients in the transverse direction; transverse transport can be both diffusive and convective. The terms Ω_T, Ω_X, and Ω_Y are reaction terms.

In order to reduce (2) to one-dimensional form, it is necessary to model the side terms in some fashion. Since the combustion field loses heat to the boundaries, we replace S_T by

$$S_T \to -\lambda(T - T_w)C_1/L^2, \tag{3}$$

where L is a length scale characterizing variations in the transverse direction. C_1 is a constant and T_w is a characteristic boundary or heat-sink temperature. In a like fashion, since on one side of the flame there is an oxygen supply boundary, and on the other a fuel-supply boundary, we write

$$S_X \to \rho D_X(X_w - X)C_2/L^2, \qquad S_Y \to \rho D_Y(Y_w - Y)C_3/L^2. \tag{4}$$

With these substitutions, (2) should be thought of as describing the evolution of averaged quantities, although the precise nature of this average is not defined. Indeed, since the side terms are not small and the two-dimensional solution is not merely a perturbation of a one-dimensional structure, the reduction to one-dimension is unavoidably *ad hoc*. It will succeed only if the replacements (3) and (4) represent the key physical contributions of the side terms.

Now it might be thought that C_1, C_2 and C_3 can be arbitrarily assigned, but that is not the case. To understand why this is so, consider a deflagration with two reactants so that, as here, there are three second-order conservation equations. Such a system has three 'eigenvalues': the propagation speed, the flame temperature, and the concentration of unburnt excess reactant behind the flame. The last two are determined by global energy conservation, and global stoichiometry.

Equations (2) also have three eigenvalues but, unlike the deflagration, the post-edge temperature and concentrations are not free variables, but are fixed by the Damköhler number. Thus, the global requirements must be satisfied some other way – specifically, constraints (two of them) on C_1, C_2 and C_3. These constraints depend on the details of the solution and on such parameters as the Lewis numbers.

Turning to the reaction terms, we note that these have unusual ingredients, *viz.*

$$\Omega_T = C_1\delta(X - X_a)(Y - Y_a)\,\mathrm{e}^{-E/RT}, \qquad \Omega_X = \gamma_x C_2\delta(X - X_a)(Y - Y_a)\,\mathrm{e}^{-E/RT},$$

$$\Omega_Y = \gamma_y C_3\delta(X - X_a)(Y - Y_a)\,\mathrm{e}^{-E/RT}. \tag{5}$$

Insight into these choices comes from examining the equilibrium states in which there is a balance between the side terms and the reaction terms, so that

$$\delta(X - X_a)(Y - Y_a)\,\mathrm{e}^{-E/RT} = \frac{\lambda(T - T_w)}{L^2Q} = \frac{\rho D_X(X_w - X)}{\gamma_X L^2} = \frac{\rho D_Y(Y_w - Y)}{\gamma_Y L^2}. \tag{6}$$

These formulas do not depend on the $\{C_j\}$ and are dependent of the speed of the edge and its structure, a necessary requirement, and one that would not be met if the $\{C_j\}$ were omitted from (5). Further, γ_X and γ_Y are stoichiometric coefficients, and are assigned constants. And X_a, Y_a are constants chosen so that the reaction is diffusion-limited for large Damköhler number ($\delta \to \infty$), and is not capped by saturation of the Arrhenius factor. That is, we specify T_a as the equilibrium temperature in the limit of infinite Damköhler number, and define X_a and Y_a by

$$\lambda\frac{(T_a - T_w)}{Q} = \frac{\rho D_X(X_w - X_a)}{\gamma_X} = \frac{\rho D_Y(Y_w - Y_a)}{\gamma_Y}. \tag{7}$$

Thus, as $\delta \to \infty$ and $T \to T_a$, the factors $(X - X_a)$ and $(Y - Y_a)$, which represent effective reactant concentrations, vanish. However, X and Y, representing average concentrations, do not. Note that the definition of T_a, X_a and Y_a is independent of the existence of an edge-flame, and our discussion is sensible, even though edge-flames can only exist over a finite band of Damköhler numbers.

The choices identified in (5) might seem curious but, once the side terms are represented by (3), (4), they are the simplest choices which preserve two key physical ingredients: that the equilibrium states (particularly the post-edge state, corresponding to the trailing diffusion flame in the underlying two-dimensional problem) be fixed by the Damköhler number δ, independently of the edge structure; and that the reaction be diffusion-limited when $\delta \to \infty$.

We now write the equations corresponding to a stationary propagating edge in non-dimensional form. In a frame attached to the edge, $\partial/\partial t \to U\partial/\partial x$ where U is the edge speed. And non-dimensional variables are defined by

$$s = x/L, \quad \theta = T/T_a, \quad V = \rho C_p L\lambda^{-1}U, \quad \bar{\delta} = C_p L^2\lambda^{-1}\,\mathrm{e}^{-1/\varepsilon}\delta, \quad \varepsilon = RT_a/E. \tag{8}$$

The governing equations then become

$$V\frac{\mathrm{d}\theta}{\mathrm{d}s} - \frac{\mathrm{d}^2\theta}{\mathrm{d}s^2} = -C_1(\theta - \theta_w) + \frac{Q}{C_pT_a}C_1\bar{\Omega},$$

$$\mathrm{Le}_X V\frac{\mathrm{d}X}{\mathrm{d}s} - \frac{\mathrm{d}^2X}{\mathrm{d}s^2} = C_2(X_w - X) - [\mathrm{Le}_X]C_2\bar{\Omega}, \tag{9}$$

$$\mathrm{Le}_Y V\frac{\mathrm{d}Y}{\mathrm{d}s} - \frac{\mathrm{d}^2Y}{\mathrm{d}s^2} = C_3(Y_w - Y) - [\mathrm{Le}_Y]C_3\bar{\Omega},$$

where

$$\bar{\Omega} = \bar{\delta}(X - X_a)(Y - Y_a)\,\mathrm{e}^{\varepsilon^{-1}(1-1/\theta)}. \tag{10}$$

The stoichiometric coefficients γ_X and γ_Y have been scaled out, and the Le_X, Le_Y in square brackets in (9b, c) can similarly be eliminated

$$(X \to \mathrm{Le}_X X, \quad X_w \to \mathrm{Le}_X X_w, \quad Y \to \mathrm{Le}_Y Y, \quad Y_w \to \mathrm{Le}_Y Y_w, \quad \bar{\delta} \to \bar{\delta}/\mathrm{Le}_X\mathrm{Le}_Y)$$

and it is in that form that we shall discuss them.

2.1. EQUILIBRIUM

We define equilibrium by setting the derivatives equal to zero, so that there is a balance between the side terms and reaction. Thus

$$\begin{aligned} -QC_p^{-1}T_a^{-1}\cdot(X - X_w) \;&=\; -QC_p^{-1}T_a^{-1}\cdot(Y - Y_w) = \theta - \theta_w \\ &= \bar{\delta}C_pT_aQ^{-1}\cdot(1-\theta)^2\,\mathrm{e}^{\varepsilon^{-1}(1-1/\theta)}. \end{aligned} \tag{11}$$

This defines an S-shaped response of θ *vs.* Damköhler number, as in Figure 1. On the top branch, when ε is small, θ is close to 1 (Figure 1 is drawn for a relatively large value of ε) and we write

$$\theta \sim 1 + \varepsilon\phi, \qquad \varepsilon \to 0, \tag{12}$$

whence

$$\phi^2\,\mathrm{e}^{\phi} = D^{-1}, \quad D = \varepsilon^2\bar{\delta}\cdot C_pT_aQ^{-1}\cdot(1-\theta_w)^{-1}. \tag{13}$$

Extinction occurs when $\phi = -2$, $D = \mathrm{e}^2/4$, *i.e.* there is no solution if $D < \mathrm{e}^2/4 (= D_e)$. If one proceeds down the S-shaped response of Figure 1, ϕ vanishes at $D = \infty$, decreases as the top branch is transversed, reaches the value (-2) at the turning point, and continues to decrease down the middle branch.

An important role is played by $O(1/\varepsilon)$ values of D, *viz.*

$$D = \varepsilon^{-1}D_1, \qquad D_1 = \varepsilon^3\bar{\delta}\cdot C_pT_aQ^{-1}\cdot(1-\theta_w)^{-1} = O(1), \tag{14}$$

whence, on the top branch,

$$\theta \sim 1 - \varepsilon\sqrt{\varepsilon}/\sqrt{D_1} + \cdots,$$
$$X \sim X_a + C_p T_a Q^{-1} \cdot \varepsilon\sqrt{\varepsilon}/\sqrt{D_1} + \cdots, \tag{15}$$
$$Y \sim Y_a + C_p T_a Q^{-1} \cdot \varepsilon\sqrt{\varepsilon}/\sqrt{D_1} + \cdots.$$

Here, D_1 is a Damköhler number that controls the equilibrium state; in particular, it controls the post-edge temperature and reactant leakage.

3. Steady asymptotic solution of an unbounded edge-flame

3.1. SOLUTION WHEN $\mathrm{Le}_X = 1, \mathrm{Le}_Y \neq 1, D_1 = O(1)(D = O(1/\varepsilon))$

In this section we examine an unbounded edge when one of the Lewis numbers differs from 1 by an $O(1)$ amount. With $\mathrm{Le}_X = 1$, we are compelled to the choice $C_2 = C_1$, and there is a Schvab–Zeldovich relation

$$X - X_w = -C_p T_a Q^{-1} \cdot (\theta - \theta_w). \tag{16}$$

How the restriction on C_2 comes about will be clear when we determine C_3.

The asymptotic structure in the limit $\varepsilon \to 0$ is similar in many respects to that of a deflagration. If the edge is located at $s = 0$, then in $s < 0$ reaction if frozen, because of the low temperature. Thus, to first order

$$s < 0\text{: } \theta = \theta_w + (1 - \theta_w)\,\mathrm{e}^{\lambda_T s}, \quad \lambda_T = \tfrac{1}{2}\sqrt{C_1} + [V/\sqrt{C_1} + \sqrt{V^2/C_1 + 4}],$$
$$Y = Y_w + (Y_a - Y_w)\,\mathrm{e}^{\lambda_Y s},$$
$$\lambda_Y = \tfrac{1}{2}\sqrt{C_3}[\mathrm{Le}_Y V/\sqrt{C_3} + \sqrt{\mathrm{Le}_Y^2 V^2/C_3 + 4}]. \tag{17}$$

Note that the equilibrium point A of Figure 1 defines the boundary conditions at $s \to -\infty$ and, with exponentially small error (see (11)), these are $\theta \to \theta_w, X \to X_w, Y \to Y_w$.

At the edge itself is located a region of intense reaction, of thickness ε. Within it there is a balance between diffusion and reaction corresponding to the asymptotic development

$$\theta = 1 + \varepsilon\phi_2 + \cdots, \qquad Y = Y_a + \varepsilon z_2 + \cdots, \qquad s = \varepsilon\xi, \tag{18}$$

where

$$\phi_2 \to 0, \qquad z_2 \to 0 \quad \text{as } \xi \to \infty \tag{19}$$

to match with (15).

In the usual way (see, for example, Buckmaster and Ludford [6, p. 21]) the gradients as $\xi \to -\infty$ can be determined, to match with the gradients defined by (17). Indeed

$$\frac{\mathrm{d}\theta}{\mathrm{d}s}(0-) = 2\sqrt{C_p T_a Q^{-1} \cdot \varepsilon^3 \bar{\delta} C_3} = -C_1 C_3^{-1} \frac{\mathrm{d}Y}{\mathrm{d}s}(0-), \tag{20}$$

whence

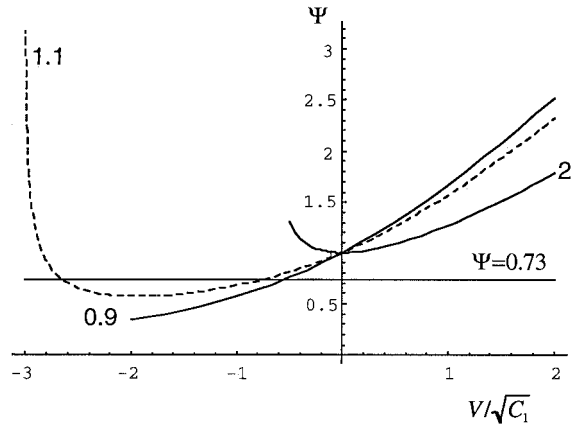

Figure 2. Variations of Ψ (proportional to the square root of the Damköhler number) with edge speed $V/\sqrt{C_1}$, when $\mathrm{Le}_X = 1$, $\mathrm{Le}_Y = 0{\cdot}9, 1{\cdot}1, 2$. The extinction value of $\Psi(0{\cdot}73)$, when $\varepsilon = \frac{1}{16}, \theta_w = 1/7$, is shown.

$$\sqrt{C_1/C_3}[V/\sqrt{C_1} + \sqrt{V^2/C_1 + 4}]$$
$$= 2\Psi = C_1 C_3^{-1}[\mathrm{Le}_Y V/\sqrt{C_3} + \sqrt{\mathrm{Le}_Y{}^2 V^2/C_3 + 4}], \tag{21}$$

where

$$\Psi = 2\sqrt{D_1}/\sqrt{1-\theta_w}. \tag{22}$$

Figure 2 shows variations of Ψ with $V/\sqrt{C_1}$ when $\mathrm{Le}_Y = 0{\cdot}9$, a response typical of these when $\mathrm{Le}_Y < 1$, the extinction value Ψ_e, of Ψ defined by the turning point of (13a), is

$$\Psi_e = \mathrm{e}\sqrt{\varepsilon}/\sqrt{1-\theta_w}, \tag{23}$$

which is $0{\cdot}73$ when $\varepsilon = 1/16, \theta_w = 1/7$. This value is shown. Figure 2 also shows responses for $\mathrm{Le}_Y = 1{\cdot}1$ and 2, both of which are characterized by a minimum value of $\Psi(\Psi_{\min})$. Such a minimum always occurs when $\mathrm{Le}_Y > 1$, and is associated with unbounded growth in Ψ as $V/\sqrt{C_1}$ approaches a critical value from above. This growth is associated with the vanishing of C_3/C_1. For values of $V/\sqrt{C_1}$ less than the critical, C_3 is negative and the solutions are unphysical. For each $\Psi > \Psi_{\min}$ there are two possible values of $V/\sqrt{C_1}$, and it is to be expected that the smaller value, lying on the portion of the response that has negative slope, corresponds to an unstable solution.

When $\mathrm{Le}_Y = 2$, Ψ achieves its minimum value of 1 when $V/\sqrt{C_1} = 0$. There is therefore a Damköhler number interval $(\frac{1}{4}\,\mathrm{e}^2 < D < (1-\theta_w)/(4\varepsilon))$ for which a post-edge structure exists, but a stationary edge structure does not; the edge-flame is necessarily unsteady. In the limit $\varepsilon \to 0$ such an interval exists for any $\mathrm{Le}_Y > 1$, but for realistic values of ε the minimum may not be reached (as $V/\sqrt{C_1}$ is decreased) before the extinction Damköhler number is reached.

3.2. $\mathrm{Le}_X = 1, \mathrm{Le}_Y = 1, D = O(1/\varepsilon)$

When $\mathrm{Le}_Y = 1$,

$$C_3 = C_1 \quad \text{and} \quad V/\sqrt{C_1} + \sqrt{V^2/C_1 + 4} = 2\Psi, \tag{24}$$

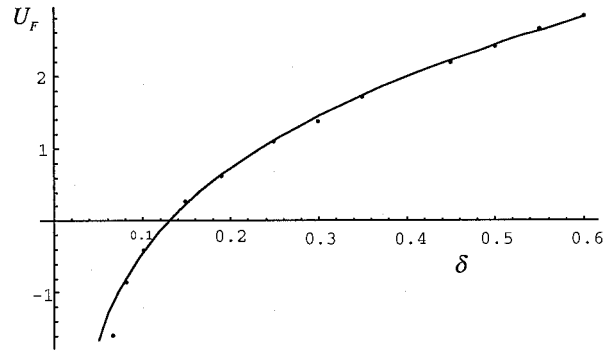

Figure 3. Edge speed (U_F) *vs.* Damköhler number (δ) from [7], and a least-squares fit omitting the left-most point.

a result obtained in [3]. It can be rewritten in the form

$$V/\sqrt{C_1} = \Psi - \Psi^{-1} \tag{25}$$

and defines a positive or negative speed accordingly as $\Psi \gtrless 1$. In the infinite Damköhler number limit $\Psi \to \infty$.

$$V \to \sqrt{C_1}\Psi \tag{26}$$

and it is natural to identify this with the adiabatic flame speed for a deflagration in a stoichiometric mixture. (That an edge-flame cannot exist in the limit is of no concern, since the ignition Damköhler number, the maximum allowable value, is exponentially large in ε).

Now an examination of (8) shows that V and Ψ are proportional to the length scale L, the length that characterizes the transverse fluxes, the side terms. Thus, for example, in the case of a flame located in a counterflow with a rate of strain α, so that $L \sim 1/\sqrt{\alpha}$, Equation (25) is equivalent to

$$U = S_L(1 - \alpha/\alpha_0), \tag{27}$$

where S_L is the dimensional flame speed, and α_0 is the value of α for which the edge speed is zero. In terms of the scalar dissipation rate, (27) is

$$U = S_L(1 - \chi/\chi_0). \tag{28}$$

With one slight exception, this is precisely the formula adopted in [5] in a discussion of lifted turbulent flames. (The exception is that χ_e, the extinction value, is used as an approximation to χ_0).

It is of interest to compare the formula (25) with numerical results obtained in [7] for the two-dimensional problem of an edge in a counterflow. Data from Figure 6 of that paper (a plot of edge speed *vs.* Damköhler number $-U_F$ *vs.* δ in the notation of [7]) is shown in Figure 3. Also shown is a least-squares fit of all the data but the left-most point using a linear combination of $\sqrt{\delta}$ and $1/\sqrt{\delta}$. (The choice of two free constants is equivalent to choosing S_L and L.) If the left-most point is retained, the fit is not so good, which is consistent with the discussion of the next Section (3.3). Also, excellent though the fit is over the restricted range

of Damköhler numbers of Figure 6 of [7], it predicts the limiting behavior $U_F \sim 4{\cdot}65\sqrt{\delta}$ as $\delta \to \infty$, compared to the value $6\sqrt{\delta}$ from the numerical data (see Figure 5 of [7]). The age of miracles is long past, and a one-dimensional model necessarily has quantative limitations.

Also shown in [7] are reaction-rate contours for a solution for which the edge speed is positive, and these reveal that reaction is sharply localized at the edge and falls off rapidly both in front of the edge and behind it. This is also a characteristic of the solution described here. Ahead of the edge reaction is frozen (exponentially small), within an $O(\varepsilon)$ neighborhood of the edge it is $O(1/\varepsilon)$, and in the post-edge equilibrium region it is $O(1)$.

Finally, before we leave this section, it is worth noting the important distinctions between the present solution and that of the classical deflagration. There is no cold-boundary difficulty, since the state at $s \to -\infty$ is defined by an equilibrium point fixed by the Damköhler number. Similarly, the flame temperature, a characteristic of the post-edge equilibrium state, is defined by the Damköhler number. The flame temperature in a deflagration is fixed by a global energy balance, and can be affected by heat losses amongst other things.

Mixing occurs ahead of the edge, but to say there is a mixture at $s \to -\infty$ is quite different from saying that there is an equilibrium point characterized by substantial reactant leakage through the reaction zone. The former will support a deflagration (an ignition wave) if ignited, whereas the latter may or may not, depending on the Damköhler number. Here the side terms play a crucial role. For a deflagration (no side terms) the preheat zone thickness ranges from 0 to ∞ as the propagation speed varies from ∞ to 0, but for the edge-flame the analogous thickness (essentially λ_T^{-1}) spans the same range for speeds varying from ∞ to $-\infty$. Decrease the Damköhler number (and so increase the thickness) in a deflagration and the speed will decrease, but always be positive. Decrease the Damköhler number in an edge-flame and the speed will become negative. For an edge-flame there is a 'watershed' value of the Damköhler number ($\Psi = 1$) for which the edge speed is zero. At larger Damköhler numbers ($\Psi > 1$) the hot post-edge flame is an ignition source for the cold mixture ahead of the edge; at smaller Damköhler numbers ($\Psi < 1$) the cold ante-edge mixture quenches the post-edge flame.

3.3. $\mathrm{Le}_X = 1, \mathrm{Le}_Y = 1, D = O(1)$

All of the discussion above is concerned with $O(1/\varepsilon)$ values of D, although edge-flames can exist for $O(1)$ values. A different asymptotic treatment is necessary in this case. Evidence for this lies in the fact that the bottom point in Figure 3, corresponding to the smallest Damköhler number in the data from [7], does not lie on the least-squares fit; and in [7], reaction contours for a solution corresponding to a significant negative edge speed show that reaction at the edge is then comparable to that in the equilibrium region behind the edge.

Since $\mathrm{Le}_Y = 1$ we have an additional Schvab–Zeldovich relation

$$Y - Y_w = -C_p T_a Q^{-1} \cdot (\theta - \theta_w) \tag{29}$$

and we have to solve an equation for θ alone, *viz.*

$$V\frac{\mathrm{d}\theta}{\mathrm{d}s} - \frac{\mathrm{d}^2\theta}{\mathrm{d}s^2} = C_1 \bar{\delta} C_p T_a Q^{-1} \cdot (1-\theta)^2\, \mathrm{e}^{\varepsilon^{-1}(1-\theta^{-1})} - C_1(\theta - \theta_w). \tag{30}$$

We seek a solution for which $\bar{\delta}\varepsilon^2 = O(1), V = O(1/\sqrt{\varepsilon}), V < 0$.

If, as before, the edge is located at $s = 0$, reaction is negligible in $s < 0$ and, because $|V|$ is large, diffusion is also negligible there. We write

$$s = -V\sigma, \tag{31}$$

whence

$$\frac{\mathrm{d}\theta}{\mathrm{d}\sigma} - C_1(\theta - \theta_w) = 0 \quad \text{in } \sigma < 0, \tag{32}$$

to first order, with solution

$$\theta = \theta_w + (1 - \theta_w)\,\mathrm{e}^{C_1\sigma}. \tag{33}$$

The edge itself is described in terms of the variables

$$\sigma = \varepsilon\xi, \qquad \theta = 1 + \varepsilon\phi(\xi), \tag{34}$$

whence

$$-\frac{\mathrm{d}\phi}{\mathrm{d}\xi} - \frac{1}{\varepsilon V^2}\frac{\mathrm{d}^2\phi}{\mathrm{d}\xi^2} = C_1(1 - \theta_x)[D\phi^2\,\mathrm{e}^{\phi} - 1]. \tag{35}$$

The boundary conditions are

$$\xi \to \infty: \quad \phi \to \phi_1 \quad \text{where} \quad D\phi_1^2\,\mathrm{e}^{\phi_1} = 1 \text{ (cf. 13)}, \tag{36}$$

$$\xi \to -\infty: \frac{\mathrm{d}\phi}{\mathrm{d}\xi} \to C_1(1 - \theta_w), \tag{37}$$

to match with the gradient of (33).

If we write

$$\frac{\mathrm{d}\phi}{\mathrm{d}\xi} = C_1(1 - \theta_w)P(\phi), \tag{38}$$

the problem reduces to a first-order equation

$$\begin{aligned} &-C_1(1 - \theta_w)\varepsilon^{-1}V^{-2} \cdot P\tfrac{\mathrm{d}P}{\mathrm{d}\phi} = P + \phi^2\phi_1^{-2}\,\mathrm{e}^{\phi - \phi_1} - 1, \\ &P(\phi_1) = 0, \qquad P(-\infty) = 1, \end{aligned} \tag{39}$$

from which the eigenvalue $\varepsilon V^2 C_1^{-1}(1-\theta_w)^{-1}$ can be determined. We are primarily concerned with the range $-2 < \phi_1 < 0$, corresponding to the upper branch, since the middle branch is unstable, but solutions to (39) can be constructed for $\phi_1 < -2$ also.

In the neighborhood of ϕ_1

$$P \sim \beta(\phi - \phi_1), \tag{40}$$

where

$$\beta = \{-1 - \sqrt{1 - 4\lambda(1 + 2/\phi_1)}\}/2\lambda, \qquad \lambda = C_1(1 - \theta_w)\varepsilon^{-1}V^{-2}, \tag{41}$$

and this can be used to specify a starting value for a shooting strategy in which λ is adjusted until the condition $P(-\infty) = 1$ is satisfied. Figure 4 shows values of λ *vs.* ϕ_1 constructed in this way. At the turning point in the $\phi_1 - D$ plane, $\lambda \simeq 1{\cdot}8$ corresponding to $-V/\sqrt{C_1} = 2{\cdot}76$,

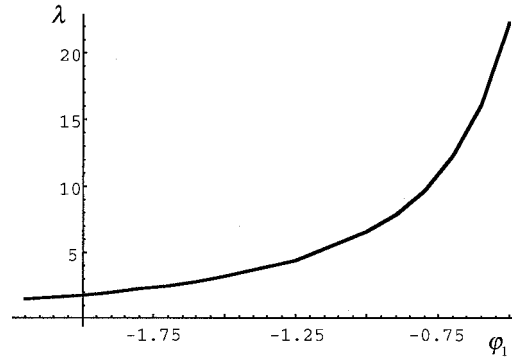

Figure 4. The eigenvalue λ *vs.* ϕ_1, defining the edge speed as a function of the post-edge temperature when $D = O(1)$.

i.e. $C_1/V^2 = 0{\cdot}13$, so that the diffusion term in the trailing flow ($\sigma < 0$) is roughly $\frac{1}{8}$ the convection term, and its neglect is plausible. The value 2·76 is significantly larger than 0·63, the value of $-V/\sqrt{C_1}$ predicted by (25) when Ψ is assigned the turning point value 0·73, so that the physics inherent in the present structure, different from that of Section 3.2, plays an important role in accelerating the edge as the Damköhler number is decreased. Figure 5 shows the variations of V with Damköhler number predicted both by the analysis of Section 3.2 and that of this section. We also show a composite formed in the usual way by adding the two values and subtracting the common term $(-1/\Psi)$ in the overlap region.

It is worth repeating that an important difference between the structure of Section 3.2 and the structure of the present section is the role played by reaction. When $D = O(1/\varepsilon)$, the reaction rate is $O(1/\varepsilon)$ within the thin edge structure, falling to $O(1)$ values behind the edge; when $D = O(1)$ the reaction rate is $O(1)$ both within and behind the edge. This distinction is evident in the two-dimensional numerical simulations of [7]. Reaction-rate contours reveal a strong maximum at the edge when $U_F = 4{\cdot}73$ (in the notation of [7]), a maximum that is significantly diminished when $U_F = 0$, and absent when $U_F = -2{\cdot}17$.

3.4. General remarks about an edge-flame in a counterflow

Dold and his colleagues, in a *tour-de-force* asymptotic analysis (albeit one with significant numerical ingredients) [8], have successfully described the response of a two-dimensional edge-flame (with $\mathrm{Le}_X = \mathrm{Le}_Y = 1$) in a counterflow. Here we shall compare the predictions of the one-dimensional model with this earlier work.

In a counterflow, the transverse length scale L is controlled by the rate of strain α and it is appropriate to make the choice

$$L = \sqrt{\lambda/(\alpha\rho C_p)}. \tag{42}$$

Then the value of α at extinction (defined by $D = \frac{1}{4}\,\mathrm{e}^2$) is

$$\alpha_e = \varepsilon^2 C_p T_a Q^{-1} \cdot (1-\theta_w)^{-1} \cdot 4\delta\,\mathrm{e}^{-1/\varepsilon}\rho^{-1}\,\mathrm{e}^{-2} \tag{43}$$

and the value of α for which $V = 0$ (defined by $\Psi = 1$) is

$$\alpha_0 = \varepsilon\,\mathrm{e}^2(1-\theta_w)^{-1}\alpha_e. \tag{44}$$

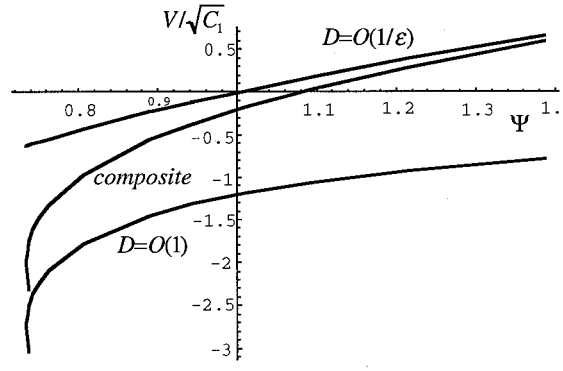

Figure 5. Variations of edge speed $V/\sqrt{C_1}$, with Ψ when $D = O(1/\varepsilon)$, $D = O(1)$, composite.

Thus $\alpha_0 = O(\varepsilon)\alpha_e$, in agreement with the two-dimensional result.

The laminar flame speed ($U = S_L$), defined by $V/\sqrt{C_1} = \Psi$, is

$$S_L/\sqrt{C_1} = 2\lambda/(\rho C_P)[\varepsilon^3(1-\theta_w)^{-2} \cdot C_p T_a Q^{-1} \cdot C_p \delta\lambda^{-1} \cdot \mathrm{e}^{-1/\varepsilon}]^{1/2}. \tag{45}$$

Thus the edge speed at the turning point ($\alpha = \alpha_e$), defined by $C_1(1-\theta_w)/(\varepsilon V^2) = 1{\cdot}8\ldots$, can be written as

$$U_e = -(1-\theta_w)\,\mathrm{e}^{-1}\varepsilon^{-1}S_L/\sqrt{1{\cdot}8} \tag{46}$$

and $U_e = O(1/\varepsilon)S_L$, which is also in agreement with the two-dimensional result.

An exception to the agreement, for which we have no definite explanation, is in the range $D_0 \lesssim D < \infty$. The one-dimensional description requires but a single formula (25) to cover the range $U = 0$ to $U = S_L$, whereas the two-dimensional description requires a dual formulation, one for which $U = O(S_L)$, and one for which $U = O(\sqrt{\varepsilon}S_L)$. A tribrachial structure is apparent in numerical simulations when D exceeds D_0 by modest amounts [7] and there are stretch affects upon the premixed branches, inherent in a two-dimensional description, which the one-dimensional model does not capture, and perhaps the reasons lie there. In this connection, however, it is worth noting that any argument, rooted in the two-dimensional picture, which attributes the retardation of an edge-flame to stretch, is misleading (albeit that stretch effects are the key ingredient in the neighborhood of the strong premixing, *i.e.* large Damköhler number, limit). The fundamental reason lies in the S-shaped response – the existence of three equilibrium solutions for a range of Damköhler numbers – an ingredient of the one-dimensional model.

A final note: when $C_1 = C_2 = C_3$, as here, there appears to be no reason why they cannot be assigned the value 1, with any uncertainties in the formulation residing in the specification of L.

3.5. Remarks on the limit $\varepsilon \to 0$

Activation-energy asyptotics has proven to be a powerful, robust tool, capable of predicting a wide variety of subtle, deep combustion phenomena. However, because physical values of ε are not particularly small, quantitive accuracy is not assured. This is undoubtedly the case here. Thus the matching between the two solutions of Figure 5 (the upper and lower curves)

is coarse. Related to this, $D_e \simeq 1{\cdot}85$ and D_0, the value for which $V/\sqrt{C_1} = 0$ (from (25)), is approximately 3·43 (when $\theta_w = 1/7, \varepsilon = 1/16$), so that asymptotically different orders of $D(D_e = O(1), D_0 = O(1/\varepsilon))$ differ only by a factor of 2 when a realistic value of ε is adopted. Qualitatively, however, the solutions that we have constructed are sensible and are, for the most part, consistent with the two-dimensional simulations of [7].

The solution of Section 3.2 has two defining characteristics: reaction is negligible when the temperature drops by more than an $O(\varepsilon)$ amount below the maximum (post-edge) value; and strong reaction is confined to a thin region in the neighborhood of the edge, where is it balanced by diffusion. These are also the characteristics of the asymptotic solution for the deflagration, and so are realistic when the edge-flame is deflagration-like (in some neighborhood of $\Psi = \infty$). The first characteristic will be realistic, even for very modest values of ε, because of the well-known effect of the exponential temperature dependence (*e.g.* $\frac{1}{4}$ is not particularly small, but e^{-4} is), and it is the second that will lose accuracy as the Damköhler number is decreased. The two-dimensional simulations suggest that this occurs when V takes on modest negative values.

The solution of Section 3.3 also has two defining characteristics: reaction quenching when the temperature drops, as before; negligible diffusion in the cold trailing flow in the ante-edge region. We have already noted that the second is reasonably satisfied at the turning point $(D = D_e)$, but it will lose accuracy as the Damköhler number is increased; it is clearly false when $V = 0$. The implication is that there is an interval of negative propagation speeds for which our solutions provide only order-of-magnitude accuracy.

4. Stagnant edge-flame near a wall

The final problem that we shall examine is that of an edge-flame located near a cold wall placed at $s = 0$ (Equations (9)) with $V = 0$. The edge is located at $s = H$, to be determined. With the scalings as before, the Lewis numbers do not appear in the equations.

Boundary conditions are

$$s = 0\text{:} \qquad \theta = \theta_w, \qquad \frac{\mathrm{d}X}{\mathrm{d}s} = 0, \qquad \frac{\mathrm{d}Y}{\mathrm{d}s} = 0. \tag{47}$$

Similarity between the X and Y descriptions mean that

$$C_2 = C_3, \qquad X - X_w = Y - Y_w. \tag{48}$$

Between the edge and the wall reaction is negligible, so that to first order

$$0 < s < H\text{:} \qquad \theta = \theta_w + (1 - \theta_w)\frac{\sinh\sqrt{C_1}s}{\sinh\sqrt{C_1}H},$$

$$X = X_w + (X_a - X_w)\frac{\cosh\sqrt{C_2}s}{\cosh\sqrt{C_2}H}. \tag{49}$$

Behind the edge $(s > H)$ equilibrium prevails and the formulas (13)–(15) are still appropriate, for, as we shall see, this problem is only meaningful when $D = O(1/\varepsilon)$.

Within the edge there is a balance between reaction and diffusion, and the 'flame-sheet' analysis familiar from deflagration studies yields formulas for the gradients to the immediate

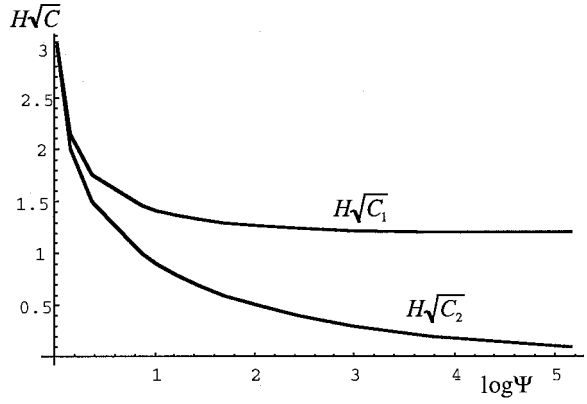

Figure 6. Variations of $H\sqrt{C_1}$ and $H\sqrt{C_2}$ with $\log\Psi$.

left of the edge ($s = H - 0$), namely

$$\frac{\mathrm{d}\theta}{\mathrm{d}s}(H-0) = \frac{C_2}{\sqrt{C_1}}\sqrt{4\frac{C_pT_a}{Q}\delta\varepsilon^3},$$

$$\frac{\mathrm{d}X}{\mathrm{d}s}(H-0) = -\frac{C_pT_a}{Q}\cdot\frac{C_2}{C_1}\frac{\mathrm{d}\theta}{\mathrm{d}s}(H-0). \tag{50}$$

These formulas are to be matched with the gradients defined by (49), whence

$$\coth\sqrt{C_1}H = \sqrt{C_1/C_2}\tanh(\sqrt{C_2})H = C_2C_1^{-1}\cdot 2\sqrt{D_1/(1-\theta_w)}. \tag{51}$$

The first of these equations is

$$\overline{H}^{-1}\coth\overline{H} = \tanh(\sqrt{\overline{C_2}}\,\overline{H})\Big/(\sqrt{\overline{C_2}}\,\overline{H}), \qquad (H\sqrt{C_1} = \overline{H}, \qquad C_2C_1^{-1} = \overline{C_2}) \tag{52}$$

and, for fixed $\overline{H}$, the right-hand side of (52) decreases monotonically from 1 to 0 as $\overline{C_2}$ is increased from 0 to ∞. There is, therefore, a single root provided $0 < \overline{H}^{-1}\coth\overline{H} \leqslant 1$, *i.e.*, $\infty > \overline{H} \geqslant 1{\cdot}199\ldots$. $\overline{C_2}$ vanishes at the limiting value $\overline{H} = 1{\cdot}199\ldots$, so that $D_1 = \infty$. And $\overline{C_2} \to 1$ as $\overline{H} \to \infty$, so that $D_1 \to \frac{1}{4}(1-\theta_w)$, the minimum Damköhler number for which there is a solution. This minimum value corresponds to $\Psi = 1$, the Damköhler number for which an unbounded edge has a zero propagation speed. Variations of $H\sqrt{C_1}$ and $H\sqrt{C_2}$ with Ψ are shown in Figure 6.

This solution makes it clear that the model has a shortcoming, since we cannot, for example, assign an arbitrary value to C_1. For, if we did, C_2 would then be fixed, yet it cannot be argued that we are better informed, *a priori*, about the nature of the side heat losses than we are about the side mass fluxes. In the absence of a closure condition then, we cannot be sure whether the limit $C_2C_1^{-1} \to 0$ should be associated with $C_2 \to 0$ or $C_1 \to \infty$; and so, in turn, we cannot be sure whether H vanishes or approaches a non-vanishing constant as $D_1 \to \infty$. This type of difficulty does not arise when $C_1 = C_2 = C_3$, as in Sections 3.2, 3.3, and it does not affect the central conclusion of Section 3.1.

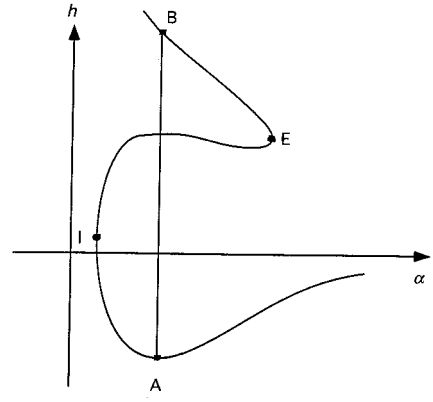

Figure 7. Flame position *vs.* rate of strain for a premixed flame in a counterflow of fresh mixture and cold inert.

5. Concluding remarks

A key characteristic of edge-flames is that they can propagate at a well-defined speed which can be of either sign. This has its roots in the S-shaped response of the underlying diffusion flame, the fact that, over a range of Damköhler numbers, there are three possible equilibria. For when $\mathrm{Le}_X = \mathrm{Le}_Y = 1$, and X, Y are linearly related to θ via Schvab-Zeldovich relations, the equation for θ is

$$V\frac{\mathrm{d}\theta}{\mathrm{d}s} - \frac{\mathrm{d}^2\theta}{\mathrm{d}s^2} = C_1 f(\theta), f(\theta) \equiv -(\theta - \theta_w) + \bar{\delta}\cdot C_p T_a Q^{-1}\cdot(1-\theta)^2\,\mathrm{e}^{\varepsilon^{-1}(1-1/\theta)}, \qquad (53)$$

whence, if $s = -\infty$ corresponds to point A in Figure 1, $s = +\infty$ to point B,

$$V\int_{-\infty}^{\infty}\left(\frac{\mathrm{d}\theta}{\mathrm{d}s}\right)^2\mathrm{d}s = C_1\int_A^B f(\theta)\,\mathrm{d}\theta. \qquad (54)$$

Since the function f has three simple zeros, one at A, one at B, and one at an intermediate value of θ, it is positive over part of the integration interval, negative over the remainder, and the sign of V depends on which part dominates.

We would expect then that edge-flames can also arise in premixed combustion, provided the underlying equilibrium function has three simple zeros. An obvious example is a premixed flame in a counterflow of cold fresh mixture and an inert whose temperature is lower than the flame-temperature. Variations of flame-position with rate of strain, for this case, are sketched in Figure 7, and the line A–B represents a transition between two stable equilibria and crosses a third, unstable equilibrium, [9]. A two-dimensional failure wave (negative edge speed) should therefore exist when B is close to the point E, and a two-dimensional ignition wave (positive edge speed) should exist when A is close to the point I.

Although edge-flames are inherently two-dimensional, we have shown in this and related papers that fundamental behavior and physical insights can be revealed by a one-dimensional model. It is of particular interest that we have been able to derive a simple formula for the edge speed as a function of the scalar dissipation rate which is, essentially, identical to the formula used in [5] in a study of lifted turbulent flames, so that the choice made by Müller *et al.* is less arbitrary than it might otherwise seem.

Another interesting prediction is that when one Lewis number is equal to 1, and the other is greater than 1, there can be a range of Damköhler numbers for which no stationary structure exists. It would be of interest to explore this with an unsteady two-dimensional numerical code.

Finally, there are unresolved issues arising from the averaging (Section 4) which, until resolved, can present difficulties of interpretation when the field variables are not similar, so that the $\{C_j\}$ are not equal.

Acknowledgment

This work was supported by AFOSR and by the NASA–Lewis Research Center.

References

1. J. W. Dold, Flame propagation in a non-uniform mixture: analysis of a slowly-varying triple-flame. *Combustion and Flame* 76 (1989) 71–88.
2. D. L. Dietrich, H. D. Ross and J. S. T'ien, Candle flames in nonbuoyant and weakly buoyant environments, paper AIAA-94-0429, 34th Aerospace Sciences Meeting, Reno, Nevada, January, 1994.
3. J. D. Buckmaster, Edge-flames and their stability. *Combustion Science and Technology* 115 (1996) 41–68.
4. J. Buckmaster and R. Weber, Edge-flame-holding, *Twenty-sixth Symposium (International) on Combustion*. Pittsburgh: The Combustion Institute (1996) to appear.
5. C. M. Müller, H. Breitbach and N. Peters, Partially premixed turbulent flame propagation in jet flames. *Twenty-fifth Symposium (International) on Combustion*. Pittsburgh: The Combustion Institute (1994) 1099–1106.
6. J. D. Buckmaster and G. S. S. Ludford, *Lectures on Mathematical Combustion*. Philadelphia: SIAM (1983) 21.
7. P. N. Kioni, B. Rogg, K. N. C. Bray and A. Liñán, Flame speed in laminar mixing layer: the triple flame. *Combustion and Flame* 95 (1993) 276–290.
8. J. W. Dold, L. J. Hartley and D. Green, Dynamics of laminar triple-flamelet structures in non-premixed turbulent combustion. In: Paul C. Fife, A. Liñán, and F. Williams (eds.), *Dynamical Issues in Combustion Theory*. New York: Springer-Verlag (1991) 83–105.
9. J. Buckmaster and D. Milkolaitis, The premixed flame in a counterflow. *Combustion and Flame* 47 (1982) 191–204.

235 259 269